Molecular Pharmacology Fast Forward. Published on October 10, 2013 as doi:10.1124/mol.113.089649

MOL #89649

Title: Identification of novel functionally selective Kappa Opioid Receptor scaffolds

Authors: Kate L. White, Alex P. Scopton, Marie-Laure Rives, Ruslan V. Bikbulatov, Prabhakar R. Polepally, Peter J. Brown, Terrance Kenakin, Jonathan A. Javitch, Jordan K. Zjawiony, Bryan L. Roth

Primary Laboratory of origin: Roth

Affiliations: The Department of Pharmacology (K.L.W., T.K., and B.L.R.), National Institute of Mental Health Psychoactive Drug Screening Program (B.L.R.), The University of North Carolina, Chapel Hill, NC. Departments of Psychiatry (M.L.R and J.A.J.) and Pharmacology (J.A.J.), Columbia University, College of Physicians and Surgeons, New York, NY. Division of Molecular Therapeutics, New York State Psychiatric Institute, New York, NY (M.L.R. and J.A.J.). The Department of Pharmacognosy, The University of Mississippi, University, MS (J.K.Z., R.V.B., and P.R.P.). Structural Genomics Consortium, University of Toronto, Toronto, ON (P.J.B. and A.S.) Current affiliation: Icahn School of Medicine at Mount Sinai, New York, NY (A.S). 36a Frontovikh Brigad Street, apt 15, Ufa, Russia 450043 (R.V.B)

Molecular Pharmacology Fast Forward. Published on October 10, 2013 as DOI: 10.1124/mol.113.089649
This article has not been copyedited and formatted. The final version may differ from this version.

Running Title: Kappa Opioid Receptor biased ligands

Corresponding Author:

Bryan L. Roth

UNC Dept. of Pharmacology

4009 Genetics Medicine CB#7365

Chapel Hill, NC 27599-7365

Tele: 919-966-7535

Fax: 919-843-5788

bryan_roth@med.unc.edu

Number of Text Pages: 21

Number of Tables: 6

Number of Figures: 2

Number of References: 48

Words in abstract: 233

Words in Introduction: 700

Words in Discussion: 1081

Abbreviations: (alphabetical)

BRET- bioluminescence resonance energy transfer

Dyn- dynorphin

GPCR- G-protein coupled receptor

KOR- kappa opioid receptor

GRK- G-protein coupled receptor kinase

Molecular Pharmacology Fast Forward. Published on October 10, 2013 as DOI: 10.1124/mol.113.089649
This article has not been copyedited and formatted. The final version may differ from this version.

Abstract

The κ opioid receptor (KOR)-dynorphin system has been implicated in the control of affect, cognition, motivation, and is thought to be dysregulated in mood and psychotic disorders, as well as in various phases of opioid dependence. KOR agonists exhibit analgesic effects although the adverse effects produced by some KOR agonists, including sedation, dysphoria, and hallucinations have limited their clinical use. Interestingly, KOR-mediated dysphoria, assessed in rodents as aversion, has recently been attributed to the activation of the p38 MAPK pathway following arrestin recruitment to the activated KOR. Therefore, KOR-selective G-protein biased agonists, which do not recruit arrestin, have been proposed to be more effective analgesics, without the adverse effects triggered by the arrestin pathway. As an initial step toward identifying novel biased KOR agonists, we applied a multi-faceted screening strategy utilizing both *in silico* and parallel screening approaches. We identified several KOR-selective ligand scaffolds with a range of signaling bias *in vitro*. The arylacetamide-based scaffold includes both G-protein and β-arrestin biased ligands, while the endogenous peptides and the diterpene scaffolds are G-protein biased. Interestingly, we found scaffold screening to be more successful than library screening in identifying biased ligands. Many of the identified functionally selective ligands are potent selective KOR agonists that are reported to be active in the central nervous system. They therefore represent excellent candidates for *in vivo* studies aiming at determining the behavioral effects mediated by specific KOR-mediated signaling cascades.

Molecular Pharmacology Fast Forward. Published on October 10, 2013 as DOI: 10.1124/mol.113.089649
This article has not been copyedited and formatted. The final version may differ from this version.

Introduction

The kappa opioid receptor (KOR)-dynorphin system has been implicated in the pathogenesis and pathophysiology of affective disorders, drug addiction, and psychotic disorders (Sheffler and Roth, 2003; Bruchas and Chavkin, 2010). KOR and dynorphin are highly expressed in regions of the brain implicated in the modulation of reward, mood, cognition and perception (ventral tegmental area, nucleus accumbens, prefrontal cortex, hippocampus, striatum, amygdala, and hypothalamus) (Land et al., 2008; Tajeda et al., 2012; Schwarzer, 2009; Knoll et al., 2010). Accordingly, drugs directed at KOR as antagonists or partial agonists have potential utility for a number of indications--especially as antidepressants and anxiolytics (Carlezon et al., 2009). Additionally, KOR agonists are gaining attention as potential anti-addiction medications and analgesics without a high abuse potential (Prevatt-Smith et al., 2011; Wee and Koob, 2010; and Tao et al., 2008). However, the adverse effects produced by many centrally-active KOR agonists, including sedation, dysphoria, and hallucinations, have limited their clinical development (Pfeiffer et al., 1986). Dysphoria has been considered the best surrogate marker of KOR agonism, while the hallucinogenic effects of KOR agonists have been relatively unexplored, except in the case of salvinorin A (Roth et al., 2002; White and Roth, 2013).

KOR stimulation leads to the activation of the canonical Gαi signaling cascade, the recruitment of β-arrestin and activation of p38 MAPK and an array of other downstream effectors (Appleyard et al., 1997; Bruchas et al., 2006; Land et al., 2009). It has been hypothesized that the dysphoric effects of KOR agonism is mediated through the arrestin-dependent activation of p38 MAPK, while the analgesic effects of KOR agonism are mediated only through G protein signaling (Bruchas et al., 2007). This suggests the potential for functionally selective ligands of KOR as analgesics devoid of dysphoric effects. Ligands that differentially stimulate canonical and non-canonical

Molecular Pharmacology Fast Forward. Published on October 10, 2013 as DOI: 10.1124/mol.113.089649
This article has not been copyedited and formatted. The final version may differ from this version.

transduction pathways are considered to be “functionally selective” (Urban et al., 2007), and their differential engagement in signaling is referred to as ‘biased’. Identifying functionally selective KOR agonists with extreme signaling bias will be useful for determining which signal transduction pathways are important for therapeutic efficacy and which signaling cascades contribute to the side effects (Allen et al., 2011). Due to the diverse structure of KOR ligands, there is the potential to discover a variety of functionally selective ligands that can be used to probe KOR signaling, as well as to improve KOR-based therapeutics. The goal of this study was to identify a range of chemotypes of functionally selective KOR ligands using a parallel *in vitro* screening approach accompanied by *in silico* selection.

KOR agonists can be classified into five chemotypes: the endogenous peptides (dynorphins), the benzodiazepines (tifluadom), the benzomorphans (ketazocine), the arylacetamides (U69593), and the diterpenes (salvinorin A). Dynorphins have been implicated in addiction and drug seeking, mood disorders, and the stress response (Bruchas and Chavkin, 2010). The benzomorphans, such as bremazocine, have limited KOR selectivity but show strong analgesic effects. However, despite their low dependence potential, they were removed from clinical development due to psychotomimetic and dysphoric effects (Dortch-Carnes and Potter, 2005). It was originally thought that the negative side effects of KOR agonists were due to off-target effects and a new class of selective KOR agonists—the arylacetamide derivatives such as U69593—was developed to circumvent these potential shortcomings. However, some arylacetamides are also reported to produce hallucinations and aversion (Millan, 1990). The diterpenes, represented by salvinorin A (which is the main psychoactive compound in *S. divinorum*), represent a novel scaffold of highly potent and selective KOR agonists with no appreciable affinity for any other known neurotransmitter system or receptor (Roth et al., 2002).

Molecular Pharmacology Fast Forward. Published on October 10, 2013 as DOI: 10.1124/mol.113.089649
This article has not been copyedited and formatted. The final version may differ from this version.

Functionally selective ligands at other targets have been identified by screening derivatives of known ligand scaffolds in a parallel fashion, in which libraries of analogues are screened simultaneously against multiple downstream effector pathways (see for instance Huang et al., 2009; Allen et al., 2011; Chen et al., 2012; Wacker et al., 2013). The extent of functional selectivity of those compounds, or bias factor, can be quantified using the operational model (Leff and Black) (Kenakin et al., 2012; Kenakin and Christopoulous, 2013; Wacker et al., 2013). Accordingly, we sought to identify and quantify the degree of bias for representative scaffolds that maintain high affinity and selectivity for KOR.

Materials and Methods:

Drugs

The NCC library used here is a publically available library consisting of FDA approved drugs we have previously used to identify biologically-active drugs (Huang et al., 2009; Huang et al., 2011). The synthesis of the RB family of salvinorin derivatives used here has been previously described: 22-chlorosalvinorin A (**RB 48**), 22-thiocyanatosalvinorin A (**RB 64**), 22-bromosalvinorin A (**RB 50**), (*22R,S*)-22-chloro-22-methylsalvinorin A (**RB-55**), (*22S*)-22-chloro-22-methylsalvinorin A (**RB 55-1**), (*22R*)-22-chloro-22-methylsalvinorin A (**RB-55-2**), 22-cyanosalvinorin A (**RB 59**), and 22-methoxysalvinorin A (**RB 65**). (Yan et al., 2009) Salvinorin A was isolated from dried leaves of *Salvia divinorum* purified as previously reported (Kutrzeba et al. 2009) and hydrolyzed to salvinorin B, which was a starting material for the synthesis of all analogs.

Dynorphin 1-13, Dynorphin 1-11, Dynorphin 1-9, Dynorphin 1-8 are all obtained from NIDA drug supply program. (+)-(5α,7α,8β)-*N*-Methyl-*N*-[7-(1-pyrrolidinyl)-1-oxaspiro[4.5]dec-8-yl]-benzeneacetamide (**U69693),** (±)-(5α,7α,8β)-3,4-dichloro-*N*-methyl-*N*-[7-(1-pyrrolidinyl)-1-oxaspiro[4.5]dec-8-yl]benzeneacetamide mesylate salt

Molecular Pharmacology Fast Forward. Published on October 10, 2013 as DOI: 10.1124/mol.113.089649
This article has not been copyedited and formatted. The final version may differ from this version.

(Spiradoline, **U62066**), 17-cyclopropylmethyl-6,7-dehydro-4,5-epoxy-3,14-dihydroxy-6,7,2',3'-indolomorphinan (**Naltrindole**), L-*N*-cyclobutylmethyl-3,14-dihydroxymorphinan (+)-tartrate salt (**Butorphanol**), and 17-(cyclobutylmethyl)-4,5-epoxymorphinan-3,6,14-triol hydrochloride hydrate (**Nalbuphine)** were purchased from Sigma-Aldrich. 4-[(3,4-Dichlorophenyl)acetyl]-3-(1-pyrrolidinylmethyl)-1-piperazinecarboxylic acid methyl ester fumarate salt (**GR89696**), 2-(3,4-dichlorophenyl)-*N*-methyl-*N*-[(1*S*)-1-phenyl-2-(1-pyrrolidinyl)ethyl]acetamide hydrochloride (**ICI199,441**), *trans*-(-)-3,4-dichloro-*N*-methyl-*N*-[2-(1-pyrrolidinyl)cyclohexyl]benzeneacetamide hydrochloride (**(-)-U50,488**), *trans*-(+)-3,4-dichloro-*N*-methyl-*N*-[2-(1-pyrrolidinyl)-cyclohexyl]benzeneacetamide hydrochloride (**(+)-U50,488**), 2-(3,4-dichlorophenyl)-*N*-methyl-*N*-[(1*S*)-1-(3-isothiocyanatophenyl)-2-(1-pyrrolidinyl)ethyl]acetamide hydrochloride (**DIPPA**), (±)-1-(3,4-dichlorophenyl)acetyl-2-(-1-pyrrolidinyl)methylpiperidine hydrochloride (**BRL 52537**), *N*-methyl-*N*-[(1*S*)-1-phenyl-2-(1-pyrrolidinyl)ethyl]phenylacetamide hydrochloride (**N-MPPP**), (*RS*)-[3-[1-[[(3,4-dichlorophenyl)acetyl]methylamino]-2-(1-pyrrolidinyl)ethyl]phenoxy]acetic acid hydrochloride (**ICI 204,448**), and Dynorphin A were purchased from Tocris. 3-(Cyclopropylmethyl)-6,11-dimethyl-1,2,3,4,5,6-hexahydro-2,6-methano-3-benzazocin-8-ol (**Cyclazocine**) and (5α,7α)-17-(cyclopropylmethyl)- 4,5-epoxy-18,19-dihydro-3-hydroxy-6-methoxy-α,α-dimethyl-6,14-ethenomorphinan-7-methanol (**Diprenorphine**) were acquired from the NIDA drug supply program.

The synthesis of *N*-naphthoyl-beta-naltrexamine (**β-NNTA)**, 6'-guanidino-17-(cyclopropylmethyl)-6,7-didehydro-4,5α-epoxy-3,14-dihydroxyindolo[2',3':6,7]morphinan (**6'-GNTI**), and 5'-Guanidino-17-(cyclopropylmethyl)-6,7-didehydro-4,5α-epoxy-3,14-dihydroxyindolo[2',3':6,7]morphinan (**5'-GNTI**) (Supplemental Methods).

Measurement of G-protein activation

A genetically engineered firefly luciferase cAMP biosensor (GloSensor; Promega) was used to quantify Gαi-mediated activity as described previously (Allen et

Molecular Pharmacology Fast Forward. Published on October 10, 2013 as DOI: 10.1124/mol.113.089649
This article has not been copyedited and formatted. The final version may differ from this version.

al., 2011; Chen et al., 2012; Wacker et al., 2013; Wu et al., 2012; Thompson et al., 2012). Details are available on-line at the NIMH Psychoactive Drug Screening Program site (http://pdsp.med.unc.edu/PDSP%20Protocols%20II%202013-03-28.pdf). In brief, HEK cells were transfected with the biosensor and KOR at a 1:1 ratio. The next day, the cells were plated into Greiner white 384-well plates (catalog # 655098). The cells were incubated with the test compound for 20-30 minutes before addition of the GloSensor™ reagent (luciferin) and isoproterenol (Allen et al., 2011). Luminescence is quantified 10 minutes after the addition of GloSensor™ reagent and isoproterenol. The Z' score for this assay using salvinorin A is 0.89 (Zhang et al., 2000).

Measurement of arrestin recruitment

Two assays were used to assess β-arrestin translocation: the Tango assay as described previously (Barnea et al., 2008; Wu et al., 2012) and a bioluminescence resonance energy transfer (BRET)-based assay as an orthologous confirmatory assay as described previously (Rives et al., 2012). The Tango assay requires the fusion of a transcription factor to the C-terminus of KOR via linker that contains a TEV protease cleavage site. Activation of KOR leads to the recruitment of β-arrestin 2 fused with TEV protease, which releases the transcription factor, making it available for induction of luciferase expression. The BRET assay requires co-transfection of KOR fused with renilla luciferase, venus tagged β-arrestin 2, and GRK 2 and the cells were distributed on 96-well plates one day prior to assay. The Z' scores using salvinorin A are 0.716 and 0.95 for the Tango assay and the BRET assay, respectively.

Virtual screening for biased ligands

Upon identification of a potential scaffold with signaling bias, we then identified analogues as detailed previously (Huang et al., 2011) using the ZINC database (Irwin et

Molecular Pharmacology Fast Forward. Published on October 10, 2013 as DOI: 10.1124/mol.113.089649
This article has not been copyedited and formatted. The final version may differ from this version.

al., 2012; Irwin and Shoichet, 2005). Compounds identified were purchased and screened as described above.

Quantifying Bias

We used the method developed by Kenakin and Christopolous to quantify the biased signaling of ligands (Kenakin et al., 2012, Kenakin and Christopoulos, 2013). After generating concentration-response curves, we fit the data to a mathematical model based on the Black and Leff Operational model to generate log(τ/KA) values. The log(τ/KA) value is a transduction coefficient that represents the affinity and efficacy of a ligand for a specific signaling pathway, in this case either G-protein activation or arrestin mobilization. This model also incorporates the receptor density and coupling within a system, and therefore is receptor expression independent. The log(τ/KA) of each test ligand is then compared to the log(τ/KA) of a reference ligand, in this case salvinorin A, for both G-protein activation and arrestin recruitment. Salvinorin A was chosen as the reference ligand because it has very similar EC_{50} values for both the G-protein and arrestin pathways and it also displays full efficacy at both pathways. Because agonists activate different signaling pathways with different efficacies and potencies, ligand bias is quantified by comparing the activity of an agonist in one assay to their relative activity in another assay, using the same reference ligand in both assays. This method reduces observation or assay bias, as well as system bias innate to the assays used (Kenakin and Christopoulos, 2013). Generating a single number that incorporates agonist affinity and efficacy is useful for identifying which ligands to use in future studies.

Results

Molecular Pharmacology Fast Forward. Published on October 10, 2013 as DOI: 10.1124/mol.113.089649
This article has not been copyedited and formatted. The final version may differ from this version.

Screening for biased ligands using G-protein activation and arrestin recruitment assays

To identify KOR ligands with signaling bias, we screened in parallel the NCC library of approved medications at a concentration of 3 μM using a split luciferase cAMP assay (Glosensor) and a genetically-encoded arrestin recruitment assay (Tango). Seven 'actives' from this screen were further analyzed by full concentration-response studies (Figure 1, Supplemental Table 1). GR89696 was the only compound from the NCC library identified as a potent biased ligand for KOR (Supplemental Table 1). The concentration-response analyses of 'actives' from the NCC library screen yielded two low potency agonists: 2-(2-aminoethyl)-pyridine and *N*-cyano-*N*'-(1,1-dimethylpropyl)-N''-3-pyridinylguanidine. Because few compounds in this library were known or predicted to bind to KOR, we continued our screening efforts with scaffolds known to have affinity for KOR. We focused on screening scaffold derivatives of arylacetamides, dynorphins, morphinans, benzomorphans, and salvinorins. Table 1.1-1.5 depicts the potencies and efficacies of these ligands for G-protein activation and arrestin mobilization (Tango) as well as the calculated bias factors.

All the arylacetamides tested are potent agonists at KOR with varying degrees of bias (Table 1.1). ICI 204,448 and BRL 52537 were identified from a virtual screen using the ZINC database (Irwin et al. 2012; Irwin and Shoichet 2005) as potentially biased ligands based on the structure of GR89696. GR89696 and ICI 199,441 displayed modest arrestin bias (bias factors 5 and 4, respectively) while ICI 204,448 and (-)U50,488 are only very weakly biased for arrestin (bias factors 2 for each compound). In contrast, U62066 and (+)U50,488 are slightly G-protein biased (bias factors 6, and 8, respectively). Lastly, we found that U69593, DIPPA, N-MPPP, and BRL 52537 are all unbiased agonists.

Molecular Pharmacology Fast Forward. Published on October 10, 2013 as DOI: 10.1124/mol.113.089649
This article has not been copyedited and formatted. The final version may differ from this version.

The dynorphin peptides tested displayed varying degrees of G-protein bias (Table 1.2). Dyn A, dyn 1-13, and dyn 1-11 have the highest degree of bias (34, 34 and 44, respectively), while dyn 1-8, dyn 1-9 are more moderately biased (4 and 16, respectively). This represents the first report of endogenous KOR ligands having a biased signaling profile relative to salvinorin A, which equally stimulates G-protein and arrestin pathways. Furthermore, the tested morphinans (Table 1.3) and benzomorphans (Table 1.4) tested displayed very little bias . Only 6' GNTI displayed a slight G-protein bias (bias factor of 6), consistent with previous studies (Rives et al., 2012 and Schmid et al., 2013). Also, we found that the antagonist JDTic has no agonistic activity in either G-protein or arrestin assays (Table 1.4).

Additionally, we tested several C-2 modified salvinorin derivatives and found them to display a wide range of G-protein bias (Table 1.5). Of this family, RB 64 and RB 48 are the most potent in activating G-protein signaling and have a high degree of bias (35 and 25, respectively). RB 59, RB 55-2, and RB 50 also have high G-protein bias factors (95, 33, and 69, respectively). RB 55-1 and RB 65 are lower potency ligands but still have a strong bias (bias factor 22 and 29, respectively). RB 55 has a slight bias factor of 8, while salvinorin B, a metabolite of salvinorin A, has a bias factor of 4.

Figure 2 depicts the G-protein activation (2A) and arrestin mobilization (2B) concentration-response curves for the compounds found to be the most potent and the most biased, along with relevant controls. The "bias plot" indicates the signaling bias of each compound by showing the response in the arrestin recruitment assay as a function of the corresponding response in the G-protein activation assay (Kenakin and Christopoulos, 2013) (Figure 2C). Thus, ICI 199,441 and GR89696 are arrestin biased, whereas RB 64 and RB 48 are G-protein biased.

Orthologous Arrestin Assay

Molecular Pharmacology Fast Forward. Published on October 10, 2013 as DOI: 10.1124/mol.113.089649
This article has not been copyedited and formatted. The final version may differ from this version.

To confirm our results from the Tango arrestin recruitment assay, we used a BRET-based arrestin-recruitment assay (Rives et al., 2012) to further analyze the compounds displaying the highest degree of bias. Salvinorin A displayed very similar potency values for the Tango and BRET assays (5.56nM and 5.63nM respectively) (Table 1 and 2). Also, the potencies of GR89696 and ICI 199,441 were very similar comparing results obtained from the Tango and BRET arrestin assays. U62066 has a slightly higher potency in the BRET assay compared to the Tango assay (19.8 nM and 6.21 nM, respectively). This shift in potency has a modest effect on the bias factor calculated with the BRET data as compared to the Tango data, but both assays suggest slight a G-protein bias for U62066 (Supplemental Table 2). Furthermore, RB 64, RB 48, RB 59, RB 55, dyn 1-13, dyn 1-9, dyn 1-11, and dyn A all have slightly higher potencies in the BRET arrestin assay than the Tango assay, while dyn 1-8 has a slightly more potent effect in Tango than BRET.

Despite modest potency differences between the Tango and BRET assays, if a ligand was identified as biased in the Tango assay then it was also identified as biased using the BRET arrestin assay. A comparison of bias factors generated from the BRET arrestin assay and the Tango assay is shown in Supplemental Table 2 and the log(τ/KA) values are listed in Supplemental Table 3.

Discussion

Recent structural evidence suggests that GPCRs adopt multiple conformations, and that different ligands can stabilize distinct conformations leading to diverse signaling profiles (Liu et al., 2012; Wacker et al., 2013; Nygaard et al., 2013; Vardy and Roth, 2013; Kenakin, 1995). Additionally, signaling partners including arrestins (Gray et al., 2003) and G-proteins (Yan et al., 2008; Nygaard et al.,2013) can allosterically modulate

Molecular Pharmacology Fast Forward. Published on October 10, 2013 as DOI: 10.1124/mol.113.089649
This article has not been copyedited and formatted. The final version may differ from this version.

agonist affinities and overall receptor conformations. This bidirectional modulation from both the ligand and the intracellular effector might affect its signaling.

In this study we sought to identify KOR selective functionally selective ligands as such ligands have been proposed to potentially function as analgesics with fewer adverse side effects (e.g. sedation and dependence). Our attempts to identify biased KOR agonists were aided by: (1) a wealth of diverse chemical matter reported to be KOR-selective; (2) assays that are both readily available and scalable; (3) and the availability of a KOR crystal structure (Wu et al., 2012). The diverse KOR chemotypes and structural information will be useful as we attempt to further optimize this structurally diverse catalogue of biased ligands. Additionally, there is increased interest in developing KOR antagonists for both depression and addiction disorders, and for developing KOR agonists as analgesics with a low abuse potential (Prevatt-Smith et al., 2011; Wee and Koob, 2010; and Yao et al., 2008). However, KOR agonists also cause aversion, hallucinations, and psychotomimetic effects (Pfeiffer et al., 1986). To develop KOR agonists that can be used as analgesics, we must understand how KOR mediates these negative side effects, and explore the use of functionally selective ligands towards KOR therapies with minimal side effects. Additionally, understanding which KOR-dependent signaling cascades mediate hallucinations will provide insight into how KOR activation affects cognition. Therefore, the first step in understanding the diverse KOR behavioral effects is to identify a range of functionally selective ligands that are potent and selective for KOR. In this study, we identify multiple centrally active KOR-selective biased ligands (RB 64, RB 48, ICI 199,441, and GR89696) that have the potential for probing KOR signaling pathways *in vivo* (Yan et al., 2009; Terner et al., 2005; Ravert et al., 2002).

Significantly, an unbiased screen of small library of known drugs yielded only a single KOR biased ligand (GR89696), although it is possible that larger screens

Molecular Pharmacology Fast Forward. Published on October 10, 2013 as DOI: 10.1124/mol.113.089649
This article has not been copyedited and formatted. The final version may differ from this version.

encompassing greater chemical diversity could yield additional scaffolds. Intriguingly, when we focused our investigation on analogues of known KOR ligands, we were able to rapidly identify additional KOR ligands with varying degrees of bias. This suggests that screening scaffold derivatives is a reliable approach for identifying biased ligands, and mirrors our results reported for D2 arrestin-biased drug discovery (Allen et al., 2011). After identifying a scaffold from the NCC screen, for instance, we tested compounds that were similar in structure to the initial arylacetamide hit. Additionally, we performed a similarity search using the ZINC database and found an additional biased ligand possessing the arylacetamide scaffold (ICI 204,448). We found arylacetamide ligands to be either weakly G-protein or arrestin biased.

We also tested varying lengths of the endogenous KOR peptide ligand, dynorphin, and found them all to be G-protein biased. Additionally, we tested the RB family of salvinorin derivatives that were originally synthesized to covalently bind to KOR. Future studies will be needed to investigate how those ligands interact with the receptor and potentially identify residues mediating the signaling bias observed. The RB family of compounds constitute the first identified KOR G-protein biased ligands that are centrally active and can therefore be used for *in vivo* probing of KOR mediated G-protein signaling (Yan et al. 2009).

To further investigate our biased ligands, we tested arrestin recruitment in an orthologous assay using bioluminescence resonance energy transfer (BRET). In general, ligands tested in the BRET assay displayed similar potencies and efficacies when compared with results obtained with the Tango assay. RB 48 and RB 59, by contrast, possess the largest differences in bias factors quantified using Tango vs. BRET assays. Notably, the incubation time is much longer for the Tango assay (16hrs) and proteolysis of the transcription factor, entry into the nucleus, transcription and translation are required downstream of arrestin recruitment whereas only arrestin recruitment is

Molecular Pharmacology Fast Forward. Published on October 10, 2013 as DOI: 10.1124/mol.113.089649
This article has not been copyedited and formatted. The final version may differ from this version.

assayed in the BRET assay (5 min). However, all ligands that we originally found to be biased using the Tango assay were also found to be biased using the BRET assay. Thus, we can infer that these compounds are functionally selective ligands for KOR –at least in HEK cells.

This is the first report of KOR-selective biased ligands that may ultimately be useful *in vivo* to discover which KOR signaling cascades are responsible for various KOR mediated behavioral effects. Although 6'-GNTI was previously identified as a biased ligand, it has a fixed charge and therefore does not readily cross the blood brain barrier (Rives et al., 2012). Additionally, while the log(τ/KA) method of quantifying bias is useful for calculating the bias *in vitro*, further studies are necessary for investigating the *in vivo* effect of these ligands as efficacies and potencies *in vitro* may not correlate with those obtained in other cell types *in vivo*. Nonetheless, using a similar strategy, we have been able to successfully advance arrestin-biased D2 agonists to *in vivo* testing and demonstrate that they retain substantial apparent bias *in vivo* (Allen et al., 2011; Chen et al., 2012).

Finally, the phenomenon of GPCR functional selectivity is not limited to arrestin mobilization and G protein activation. For example, we have identified 5-HT_{2A} inverse agonists which can induce receptor internalization and down-regulation *in vitro* and *in vivo* without activating ***either*** G-protein signaling or arrestin translocation (Bhatnagar et al., 2001; Xia et al., 2003; Yadav et al., 2011). In future studies, it will be useful to combine *in vivo* behavioral studies and a global study of intracellular signaling with functionally selective ligands, in order to fully understand which signaling cascades contribute to the various behavioral effects of KOR agonism. The present study suggests that simply screening available scaffolds represents a facile method for identifying functionally selective ligands with good drug-like properties. The rapid increase in GPCR

Molecular Pharmacology Fast Forward. Published on October 10, 2013 as DOI: 10.1124/mol.113.089649
This article has not been copyedited and formatted. The final version may differ from this version.

structural and dynamic information, and our expanded understanding of functional selectivity, has enhanced the potential for designing more selective therapies with fewer side effects for a multitude of diseases and conditions. In the future, screening compounds for a more global activation of pathways in addition to those activated by G-proteins should allow for a better understanding of how these ligands affect physiology, and how functionally selective compounds might have beneficial therapeutic value.

Acknowledgments:

We thank Dr. Wesely K. Kroeze for critically reading this manuscript and NIDA for the supply of dynorphin peptides.

Author Contributions:

Participated in research design: White and Roth

Conducted experiments: White

Contributed compounds, tools, and protocols: Bikbulatov, Polepally, Zjawiony, Rives, Javitch, Scopton, Brown

Assisted with data analysis and interpretation: White, Roth, Kenakin, Rives, Javitch

Wrote or contributed to writing the manuscript: White, Roth, Rives, and Javitch

Molecular Pharmacology Fast Forward. Published on October 10, 2013 as DOI: 10.1124/mol.113.089649
This article has not been copyedited and formatted. The final version may differ from this version.

References:

Allen JA, Yost JM, Setola V, Chen X, Sassano MF, Chen M, Peterson S, Yadav PN, Huang XP, Feng B, Jensen NH, Che X, Bai X, Frye SV, Wetsel WC, Caron MG, Javitch JA, Roth BL, Jin J. (2011) Discovery of beta-arrestin-biased dopamine D2 ligands for probing signal transduction pathways essential for antipsychotic efficacy. *Proc Natl Acad Sci USA*. **108**(45)18488-184893.

Appleyard SM, Patterson TA, Jin W, Chavkin C. (1997) Agonist-induced phosphorylation of the kappa-opioid receptor. *J Neurochem*. **69**(6):2405-2412.

Barnea G, Strapps W, Herrada G, Berman Y, Ong J, Kloss B, Axel R, Lee KJ. (2008) The genetic design of signaling cascades to record receptor activation. *Proc Natl Acad Sci USA*. **105**(1):64-69.

Bhatnagar A, Willins DL, Gray JA, Woods J, Benovic JL, Roth BL. (2001) The dynamin-dependent, arrestin-independent internalization of 5-hydroxytryptamine 2A (5-HT2A) serotonin receptors reveals differential sorting of arrestins and 5-HT2A receptors during endocytosis. *J Biol Chem.* **276**(11):8269-8277.

Bruchas MR, Macey TA, Lowe JD, Chavkin C. (2006) Kappa opioid receptor activation of p38 MAPK is GRK3- and arrestin-dependent in neurons and astrocytes. *J Biol Chem*. **281**(26):18081-18089.

Bruchas MR, Land BB, Aita M, Xu M, Barot SK, Li S, Chavkin C. (2007) Stress-induced p38 mitogen-activated protein kinase activation mediates kappa-opioid-dependent dysphoria. *J Neurosci*. **27**(43):11614-11623.

Bruchas MR and Chavkin C. (2010) Kinase cascades and ligand-directed signaling at the kappa opioid receptor. *Psychopharmacology (Berl)*. **210**(2):137-147.

Carlezon WA Jr, Beguin C, Knoll AT, Cohen BM. (2009) Kappa-opioid ligands in the study and treatment of mood disorders. *Pharmacol Ther.* **123**(3):334-343.

Chen X, Sassano MF, Zheng L, Setola V, Chen M, Bai X, Frye SV, Wetsel WC, Roth BL, Jin J. (2012) Structure-functional selectivity relationship studies of beta-arrestin-biased dopamine D2 receptor agonists. *J Med Chem*. **55**(16): 7141-7153.

Dortch-Carnes J and Potter DE. (2005) Bremazocine: a kappa-opioid agonist with potent analgesic and other pharmacological properties. *CNS Drug Rev*. **11**(2):195-212.

Gray JA, Bhatnagar A, Gurevich W, Roth BL. (2003) The interaction of a consitutively active arrestin with the arrestin-insensitive 5-HT(2A) receptor induces agonist-independent internalization. *Mol Pharmacol.* **63**(5):961-972

Huang XP, Setola V, Yadav PN, Allen JA, Rogan SC, Hanson BJ, Revankar C, Robers M, Doucette C, Roth BL. (2009) Parallel functional activity profiling reveals valvulopathogens are potent 5-hydroxytryptamine (2B) receptor agonists: implications for drug safety assessment. *Mol Pharmacol.* **76**(4):710-722.

Huang HS, Allen JA, Mabb AM, King IF, Miriyala J, Taylor-Blake B, Sciaky N, Dutton JW Jr, Lee HM, Chen X, Jin J, Bridges AS, Zylka MJ, Roth BL, Philpot BD. (2011)

Topoisomerase inhibitors unsilence the dormant allele of Ube3a in neurons. *Nature*. **481**(7380):185-189.

Irwin JJ and Shoichet BK. (2005) ZINC—a free database of commercially available compounds for virtual screening. *J Chem Inf Model.* **45**(1):177-182.

Irwin JJ, Sterling T, Mysinger MM, Bolstad ES, Coleman RG. (2012) ZINC: A free tool to discover chemistry for biology. *J Chem Inf Model.* **52**(7):1757-1768.

Kenakin T. (1995) Agonist-receptor efficacy. II. Agonist trafficking of receptor signals. *Trends Pharmacol Sci.* **16**(7):232-238.

Kenakin T, Watson C, Muniz-Medina V, Christopoulos A, Novick S. (2012) A simple method for quantifying functional selectivity and agonist bias. *ACS Chem Neurosci.* **3**(3):193-203.

Kenakin T and Christopoulos A. (2013) Signalling bias in new drug discovery: detection, quantification and therapeutic impact. *Nat Rev Drug Discov.* **12**(3):205-216.

Knoll AT and Carlezon WA Jr. (2010). Dynorphin, stress, and depression. *Brain Res*. **1314**:56-73.

Kutrzeba LM, Karamayan VT, Speth RC, Williamson JS, Zjawiony JK. (2009) *In vitro* studies on metabolism of salvinorin A. *Pharm. Biol.* **47**(11):1078-1084.

Land BB, Bruchas MR, Lemos JC, Xu M, Melief EJ, Chavkin C. (2008) The dysphoric component of stress is encoded by activation of the dynorphin kappa-opioid system. *J. Neurosci*. **28**(2):407-414.

Land BB, Bruchas MR, Schattauer S, Giardino WJ, Aita M, Messinger D, Hnasko TS, Palmiter RD, Chavkin C. (2009) Activation of the kappa opioid receptor in the dorsal raphe nucleus mediates the aversive effects of stress and reinstates drug seeking. *Proc Natl Acad Sci USA*. **106**(45):19168-19173.

Liu JJ, Horst R, Katritch V, Stevens RC, Wuthrich K. (2012) Biased signaling pathways in beta(2)-adrenergic receptor characterized by 19F-NMR. *Science*. **335**(6072):1106-1110.

Millan MJ. (1990) Kappa-opioid receptors and analgesia. *Trends Pharmacol Sci.* **11**(2):70-76.

Nygaard R, Zou Y, Dror RO, Mildorf TJ, Arlow DH, Manglik A, Pan AC, Liu CW, Fung JJ, Bokoch MP, Thian FS, Kobilka TS, Shaw DE, Mueller L, Prosser RS, Kobilka BK. (2013) The dynamic process of beta(2)-adrenergic receptor activation. *Cell.* **152**(3):532-542.

Pfeiffer A, Brantl V, Herz A, Emrich HM. (1986) Psychotomimesis mediated by kappa opiate receptors. *Science*. **233**(4765):774-776.

Prevatt-Smith KM, Lovell KM, Simpson DS, Day VW, Douglas JT, Bosch P, Dersch CM, Rothman RB, Kivell B, Prisinzano TE. (2011) Potential drug abuse therapeutics derived from the halluncinogenic natural product salvinorin A. *Medchemcomm*. **2**(12):1217-1222.

Ravert HT, Scheffel U, Mathews WB, Musachio JL, Dannals RF. (2002) [^{11}C]-GR89696, a potent kappa opiate receptor radioligand; *in vivo* binding of the R and S enantiomers. *Nucl med Biol.* **29**(1):47-53.

Rives ML, Rossillo M, Liu-Chen LY, Javitch JA. (2012) 6'-Guanidinonaltrindole (6'-GNTI) is a G protein-biased kappa-opioid receptor agonist that inhibits arrestin recruitment. *J Biol Chem.* **287**(32):27050-27054.

Roth BL, Baner K, Westkaemper R, Siebert D, Rice KC, Steinberg S, Ernsberger P, Rothman RB. (2002) Salvinorin A: a potent naturally occurring nonnitrogenous kappa opioid selective agonist. *Proc Natl Acad Sci USA*. **99**(18):11934-11939.

Schmid CL, Streicher JM, Groer CE, Munro TA, Zhou L, Bohn LM. (2013) Functional Selectivity of 6'-Guanidinonaltrindole (6'-GNTI) at kappa-opioid receptors in striatal neurons. **288**(31):22387-22398.

Schwarzer C. (2009) 30 years of dynorphins—new insights on their functions in neuropsychiatric diseases. *Pharmacol Ther.* **123**(3):353-370.

Sheffler DJ and Roth BL. (2003) Salvinorin A: the "magic mint" hallucinogen finds a molecular target in the kappa opioid receptor. *Trends Pharmacol Sci*. **24**(3):107-109.

Tajeda HA, Shippenberg TS, Henriksson R. (2012) The dynorphin/kappa-opioid receptor system and its role in psychiatric disorders. *Cell Mol Life Sci.* **69**(6):857-896.

Tao Y-M, Li Q-L, Zhang C-F, Xu X-J, Chen J, Ju Y-W, Chi Z-Q, Long Y-Q, Liu J-G. (2008) LPK-26, a novel kappa-opioid receptor agonist with potent antinociceptive effects and low dependence potential. *Eur J Pharmacol.* **584**(2-3):306-311.

Terner JM, Lomas LM, Lewis JW, Husbands SM, Picker MJ. (2005) Effects of the long-lasting kappa opioid 2-(3,4-dichlorophenyl)-N-methyl-N[(1S)-1-(3-isothiocyanatophenyl)-2-(1-pyrrolidinyl) ethyl] acetamide in a drug discrimination and warm water tail-withdrawal procedure. *Behav Pharmacol.* **16**(8):665-670.

Thompson AA, Liu W, Chun E, Katritch V, Wu H, Vardy E, Huang XP, Trapella C, Guerrini R, Calo G, Roth BL, Cherezov V, Stevens RC. (2012) Structure of the nociception/orphanin FQ receptor in complex with a peptide mimetic. *Nature*. **485**(7398):395-399.

Urban JD, Clarke WP, von Zastrow M, Nichols DE, Kobilka B, Weinstein H, Javitch JA, Roth BL, Christopoulos A, Sexton PM, Miller KJ, Spedding M, Mailman RB. (2007) Functional selectivity and classical concepts of quantitative pharmacology. *J Pharmacol Exp Ther.* **320**(1):1-13.

Vardy E. and Roth BL. (2013) Conformational ensembles in GPCR activation. *Cell.* **152**(3):385-386.

Wacker D, Wang C, Katritch V, Han GW, Huang XP, Vardy E, McCorvy JD, Jiang Y, Chu M, Siu FY, Liu W, Xu HE, Cherezov V, Roth BL, Stevens RC. (2013) Structural features for functional selectivity at serotonin receptors. *Science.* **340**(6132):615-619.

Wee S and Koob GF. (2010) The role of the dynorphin-kappa opioid system in the reinforcing effects of drugs of abuse. *Psychopharmacology (Berl).* **210**(2):121-135.

White KL and Roth BL. (2012) Psychotomimetic effects of kappa opioid receptor agonists. *Biol Psychiatry*. **72**(10):797-798.

Wu H, Wacker D, Mileni M, Katritch V, Han GW, Vardy E, Liu W, Thompson AA, Huang XP, Carroll FI, Mascarella SW, WEstkaemper RB, Mosier PD, Roth BL, Cherezov V, Stevens RC. (2012) Structure of the human kappa-opioid receptor in complex with JDTic. *Nature.* **485**(7398):327-332.

Yadav PN, Kroeze WK, Farrell MS, Roth BL. (2011) Antagonist functional selectivity: 5-HT2A serotonin receptor antagonists differentially regulate 5-HT2A receptor protein level in vivo. *J Pharmacol Exp Ther.* **339**(1):99-105.

Yan F, Mosier PD, Westkaemper RB, Roth BL. (2008) Galpha-subunits differentially alter the conformation and agonist affinity of kappa-opioid receptors. *Biochemistry.* **47**(6):1567-1578.

Yan F, Bikbulatov RV, Mocanu V, Dicheva N, Parker CE, Wetsel WC, Mosier PD, Westkaemper RB, Allen JA, Zjawiony JK, Roth BL. (2009) Structure-based design, synthesis, and biochemical and pharmacological characterization of novel salvinorin A analogues as active state probes of the kappa-opioid receptor. *Biochemistry*. **48**(29):6898-6908.

Xia Z, Gray JA, Compton-Toth BA, Roth BL. (2003) A direct interaction of PSD-95 with 5-HT2A serotonin receptors regulates receptor trafficking and signal transduction. *J Biol Chem*. **278**(24):21901-21908.

Zhang, J.H., Chung, T.D.Y. & Oldenburg, K.R. (2000) Confirmation of primary active substances from high throughput screening of chemical and biological populations: a statistical approach and practical considerations. *J. Comb. Chem.* **2**(3): 258–265.

Molecular Pharmacology Fast Forward. Published on October 10, 2013 as DOI: 10.1124/mol.113.089649
This article has not been copyedited and formatted. The final version may differ from this version.

Footnotes:

A.) Funding sources:

The work was funded by the National Institute of Health [RO1DA01724; U19MH82441; K05 DA022413; R01 MH54137], a National Institute on Drug Abuse EUREKA Grant, and the National Institute of Mental Health Psychoactive Drug Screening Program. The Structural Genomics Consortium is a registered charity (number 1097737) that receives funds from AbbVie, Boehringer Ingelheim, the Canada Foundation for Innovation, the Canadian Institutes for Health Research, Genome Canada through the Ontario Genomics Institute [OGI-055], GlaxoSmithKline, Janssen, Lilly Canada, the Novartis Research Foundation, the Ontario Ministry of Economic Development and Innovation, Pfizer, Takeda, and the Wellcome Trust [092809/Z/10/Z].

B) Citation of meeting abstracts where the work was previously presented:

White KL, Vardy E, Roth BL. (2013) Utilizing functionally selective ligands to probe specific signaling pathways of the kappa opioid receptor. Kappa Therapeutics 2013, Cambridge MA.

C.) For reprint requests contact:

Bryan L. Roth

UNC Dept. of Pharmacology

4009 Genetics Medicine CB#7365

Chapel Hill, NC 27599-7365

Tele: 919-966-7535

Fax: 919-843-5788

bryan_roth@med.unc.edu

Molecular Pharmacology Fast Forward. Published on October 10, 2013 as DOI: 10.1124/mol.113.089649
This article has not been copyedited and formatted. The final version may differ from this version.

Figure Legends

Figure 1. **NCC library screening results.**

A.) Depiction of the parallel screening approach used. B.) Scatter plot showing the results of the screening of the NCC library in the arrestin assay. **1**: Bestatin; **2**:GR8969; **3**: 2-(2-aminoethyl) pyridine; **4**: *N*-cyano-*N*'-(1,1-dimethylpropyl)-N''-3-pyridinylguanidine; **5**: Brucine; **6**: Doxapram; **7**: Diphenoxylate.

Figure 2. Arrestin mobilization and G-protein activation dose response curves of candidates for *in vivo* studies.

The dose-response curves of candidate ligands for arrestin recruitment measured via Tango (A), G-protein activation (B), and the bias plot (C). These ligands all have similar potency and efficacy values for G-protein signaling, yet the potency values for arrestin mobilization differ greatly. The bias plot highlights the differences in potency and efficacy values for each ligand in both G-protein and arrestin pathways.

Molecular Pharmacology Fast Forward. Published on October 10, 2013 as DOI: 10.1124/mol.113.089649
This article has not been copyedited and formatted. The final version may differ from this version.

Table 1.1. Affinity and potency values for arylacetamides using GloSensor and Tango

Arylacetamides	G-protein EC_{50}	G-protein Emax	Arrestin EC_{50}	Arrestin Emax	Bias Factor
Salvinorin A	5.183 nM (-8.29 +/-0.10)	99.7	5.75 nM (-8.24 +/-0.06)	97.2	1
ICI 199,441	1.63 nM (-8.79 +/-0.07)	101	0.428 nM (-9.37+/- 0.05)	84.8	4 **Arrestin**
ICI 204,448	4.22 nM (-8.38 +/-0.09)	111	3.28nM (-8.48+/-0.06)	77.4	2 **Arrestin**
U69593	5.89 nM (-8.23 +/-0.07)	109	6.42 nM (-8.19 +/-0.09)	89.3	1
GR89696	0.970 nM (-9.01 +/-0.11)	96.4	0.259 nM (-9.60+/-0.06)	92.8	5 **Arrestin**
U62066	1.01 nM (-9.00 +/-0.05)	103	6.21 nM (-8.21 +/-0.10)	92.7	6 **G-protein**
(+) U50,488	246 nM (-6.61 +/-0.12)	102	959 nM (-6.02 +/-0.08)	92.3	8 **G-protein**
(-) U50,488	0.858 nM (-9.06+/-0.07)	95.5	0.822nM (-9.09+/-0.09)	94.6	2 **Arrestin**
DIPPA	14.5 nM (-7.84+/-0.09)	111	8.49 nM (-8.07 +/-0.07)	68.5	1
N-MPPP	4.45 nM (-8.35 +/-0.09)	109	2.41 nM (-8.62 +/-0.06)	79.7	1
BRL 52537	1.85 nM (-8.73 +/-0.07)	112	1.35 nM (-8.87 +/-0.05)	88.9	1

Molecular Pharmacology Fast Forward. Published on October 10, 2013 as DOI: 10.1124/mol.113.089649
This article has not been copyedited and formatted. The final version may differ from this version.

Table 1.2. Affinity and potency values for dynorphin peptides using GloSensor and Tango assays

Peptides	G-protein EC_{50}	G-protein Emax	Arrestin EC_{50}	Arrestin Emax	Bias Factor
Salvinorin A	5.183 nM (-8.29 +/-0.10)	99.7	5.75 nM (-8.24 +/-0.06)	97.24	1
Dynorphin A	8.12 nM (-8.09 +/-0.07)	101	268 nM (-6.57 +/-0.11)	74.8	34 **G-protein**
Dyn 1-8	57.7 nM (-7.24 +/-0.05)	106	720 nM (-6.14+/-0.11)	89.9	4 **G-protein**
Dyn 1-9	10.2nM (-7.99+/-0.06)	101	600nM (-6.22+/-0.09)	64.7	16 **G-protein**
Dyn 1-11	3.26nM (-8.49+/-0.08)	101	450nM (-6.35 +/-0.09)	75.8	44 **G-protein**
Dyn 1-13	2.07nM (-8.68+/-0.07)	96.6	97.8nM (-7.01 +/-0.07)	72.4	34 **G-protein**

Molecular Pharmacology Fast Forward. Published on October 10, 2013 as DOI: 10.1124/mol.113.089649
This article has not been copyedited and formatted. The final version may differ from this version.

Table 1.3. Affinity and potency values for morphinans using GloSensor and Tango assays

Morphinans	G-protein EC_{50}	G-protein Emax	Arrestin EC_{50}	Arrestin Emax	Bias Factor
Salvinorin A	5.18 nM (-8.29 +/-0.10)	99.7	5.75 nM (-8.24 +/-0.06)	97.2	1
β-NNTA	0.305 nM (-9.52+/-0.12)	97.0	0.268 nM (-9.57+/-0.12)	84.5	1
6' GNTI	4.74 nM (-8.32 +/-0.09)	96.5	7.38 nM (-8.13 +/-0.12)	34.7	6 **G-protein**
5' GNTI	Antagonist	-	Antagonist	-	

Molecular Pharmacology Fast Forward. Published on October 10, 2013 as DOI: 10.1124/mol.113.089649
This article has not been copyedited and formatted. The final version may differ from this version.

Table 1.4. Affinity and potency values for benzomorphans using GloSensor and Tango assays

Benzomorphans	G-protein EC_{50}	G-protein Emax	Arrestin EC_{50}	Arrestin Emax	Bias Factor
Salvinorin A	3.63nM (-8.29 +/- 0.10)	103	6.67nM (-8.18+/-0.05)	99.42	1
Naltrindole	Antagonist	-	Antagonist	-	
Diprenorphine	0.960 nM (-9.02 +/-0.08)	88.3	3.35 nM (-8.48 +/-0.14)	87.0	2 **G-protein**
Nalbuphine	61.5 nM (-7.21 +/-0.11)	81.3	47.2 nM (-7.33+/-0.08)	74.1	3 **Arrestin**
Butorphanol	1.82 nM (-8.74 +/-0.07)	94.3	1.70nM (-8.77+/-0.06)	59.2	2 **G-protein**
Cyclazocine	1.19 nM (-8.92 +/-0.09)	102	0.806nM (-9.09+/-0.03)	81.7	1
JDTic	Antagonist	-	Antagonist	-	

Molecular Pharmacology Fast Forward. Published on October 10, 2013 as DOI: 10.1124/mol.113.089649
This article has not been copyedited and formatted. The final version may differ from this version.

Table 1.5. Affinity and potency values for RB family of salvinorin derivatives using GloSensor and Tango assays

RB **Salvinorins**	G-protein EC_{50}	G-protein Emax	Arrestin EC_{50}	Arrestin Emax	Bias Factor G-protein
Salvinorin A	5.183 nM (-8.29 +/-0.10)	99.7	5.75 nM (-8.24+/-0.06)	97.2	1
Salvinorin B	73.4 nM (-7.13 +/-0.08)	95.9	428 nM (-6.37+/-0.07)	115	4 **G-protein**
RB-64	5.29 nM (-8.27 +/-0.06)	101	391 nM (-6.41 +/-0.05)	104	35 **G-protein**
RB-48	8.82 nM (-8.05+/- 0.07)	101	143 nM (-6.84 +/-0.09)	63.2	25 **G-protein**
RB-55_1	119nM (-6.93+/- 0.07)	101	1492 nM (-5.83 +/-0.15)	52.2	22 **G-protein**
RB-55_2	142 nM (-6.84+/- 0.10)	105	2284 nM (-5.64 +/-0.09)	56.8	33 **G-protein**
RB 55	31.3 nM (-7.50+/-0.08)	103	229 nM (-6.64 +/-0.07)	86.9	8 **G-protein**
RB 50	166 nM (-6.78+/- 0.10)	103	3812 nM (-5.42+/-0.21)	89.2	69 **G-protein**
RB 59	35.8 nM (-7.45+/-0.10)	95.7	4290 nM (-5.37+/-0.13)	76.6	95 **G-protein**
RB 65	145 nM (-6.83+/-0.10)	95.9	2767 nM (-5.56+/-0.13)	42.7	29 **G-protein**

Molecular Pharmacology Fast Forward. Published on October 10, 2013 as DOI: 10.1124/mol.113.089649
This article has not been copyedited and formatted. The final version may differ from this version.

Table 2. BRET arrestin affinity and potency values

Compound	EC50	Emax
Salvinorin A	5.55 nM (-8.25+/-0.05)	98.84
GR89896	0.265 nM (-9.58+/-0.03)	104
ICI 199,441	0.461 nM (-9.34+/-0.07)	100
U62066	19.8 nM (-7.70+/-0.07)	101
RB 64	118nM (-6.93+/-0.06)	105
RB 48	45.0nM (-7.35+/-0.06)	101
RB 55	196nM (-6.71+/-0.03)	78.9
RB 59	3560 nM (-5.44+/-0.18)	177
Dyn 1-13	78.2 nM (-7.11+/-0.13)	86.3
Dyn 1-11	132 nM (-6.87+/-0.16)	86.9
Dyn 1-9	253 nM (-6.59+/-0.11)	92.8
Dyn 1-8	1070 nM (-5.97+/-0.11)	102
Dynorphin A	112 nM (-6.95+/-0.13)	99.2

Figure 1

A.

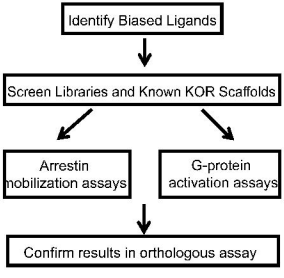
Identify Biased Ligands
Screen Libraries and Known KOR Scaffolds
Arrestin mobilization assays
G-protein activation assays
Confirm results in orthologous assay

B.

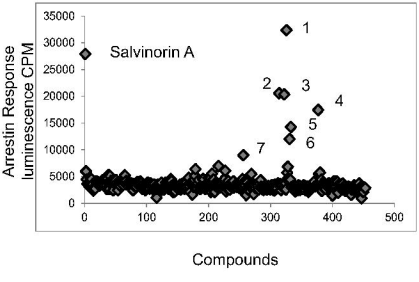
Arrestin Response luminescence CPM
Compounds
Salvinorin A
1
2
3
4
5
6
7
35000
30000
25000
20000
15000
10000
5000
0
0
100
200
300
400
500

Figure 2

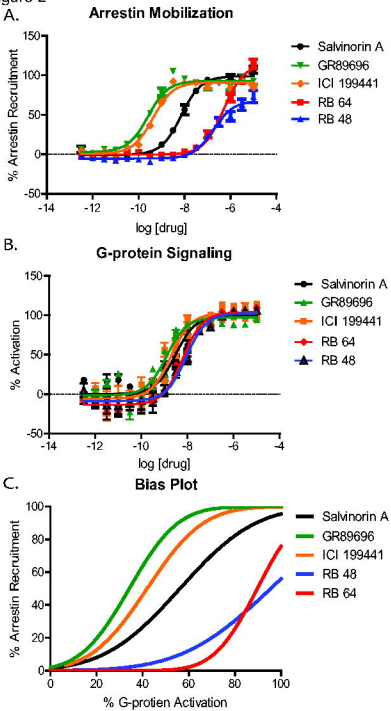
A.
Arrestin Mobilization
% Arrestin Recruitment
log [drug]
Salvinorin A
GR89696
ICI 199441
RB 64
RB 48
B.
G-protein Signaling
% Activation
log [drug]
Salvinorin A
GR89696
ICI 199441
RB 64
RB 48
C.
Bias Plot
% Arrestin Recruitment
% G-protien Activation
Salvinorin A
GR89696
ICI 199441
RB 48
RB 64

Supplemental Data

Molecular Pharmacology

Identification of novel functionally selective Kappa Opioid Receptor scaffolds

Kate L. White, Alex P. Scopton, Marie-Laure Rives, Ruslan V. Bikbulatov, Prabhakar R. Polepally, Peter J. Brown, Terrance Kenakin, Jonathan A. Javitch, Jordan K. Zjawiony, Bryan L. Roth

Supplemental table 1 legend.

GR89696 was identified as a potent agonist for KOR for both G-protein activation and arrestin mobilization. However, GR89696 is more potent in activating arrestin than G-protein relative to salvinorin A. This compound was the only potent functionally selective ligand identified in the NCC library. Brucine, Doxapram, and Diphenoxylate show some activity at higher doses (1uM and higher) but do not generate reliable dose response curves.

Supplemental Table 1. Functional results from hits from NCC library

Compound	G-Protein EC_{50}	Emax	Arrestin EC_{50}	Emax
GR8969	0.515nM (-9.29 +/-0.11)	95.38	0.25nM (-9.60+/-0.06)	93.92
Bestatin	-	-	-	-
2-(2-aminoethyl) pyridine	1050nM (-5.98+/-0.68)	184	550nM (-6.26+/-0.09)	110
N-cyano-*N*'-(1,1-dimethylpropyl)-N''-3-pyridinylguanidine	159nM (-6.81+/-0.34)	85.0	233nM (-6.63+/-0.32)	73
Doxapram	-	-	-	-
Brucine	-	-	-	-
Diphenyoxylate	-	-	-	-

Supplemental Table 2. Comparison of Bias Factor and EC_{50} generated with Tango and BRET assays

Compound	EC_{50} and Emax GloSensor	EC_{50} and Emax Tango	EC_{50} and Emax BRET	Bias Factor (Tango)	Bias Factor (BRET)
Salvinorin A	5.18 nM 99.7	5.75 nM 97.2	5.54 nM 98.8	1	1
GR89696	0.970 nM 96.4	0.259 nM 92.8	0.265 nM 104	5 Arrestin	5 Arrestin
ICI 199,441	1.63 nM 101	0.428 nM 84.8	0.461 nM 100	4 Arrestin	4 Arrestin
U62066	1.01 nM 103	6.21 nM 92.3	19.8 nM 101	6 G-Protein	18 G-Protein
RB 64	5.29 nM 102	391 nM 103	118 nM 105	35 G-Protein	13 G-Protein
RB 48	8.82 nM 101	143 nM 63.2	45.0 nM 101	25 G-Protein	4 G-Protein
RB 55	31.3 nM 103	229 nM 86.9	196 nM 79.0	8 G-Protein	10 G-Protein
RB 59	35.8 nM 95.7	4290 nM 76.6	3560 nM 177	95 G-Protein	35 G-Protein
Dyn 1-13	2.07 nM 96.6	97.8 nM 72.4	78.2 nM 86.3	34 G-Protein	32 G-Protein
Dyn 1-11	3.26 nM 101	450 nM 75.8	253 nM 92.0	44 G-Protein	27 G-Protein
Dyn 1-9	10.2 nM 101	600 nM 64.6	132 nM 86.9	16 G-Protein	15 G-Protein
Dyn 1-8	57.7 nM 106	720 nM 89.9	1068 nM 103	4 G-Protein	8 G-Protein
Dyn A	8.12 nM 101	268 nM 74.8	112 nM 99.2	34 G-Protein	20 G-Protein

Supplemental Table 3. LogTau/KA values for all ligands tested

Drug	LogTau/KA GloSensor	LogTau/KA Tango	LogTau/KA BRET
Salvinorin A	8.197 +/-0.08	8.175 +/-0.07	8.182 +/-0.04
U69593	8.140 +/-0.08	8.126 +/-0.06	
(+) U50488	6.783 +/-0.09	5.873 +/-0.09	
U62066	8.979 +/-0.09	8.173 +/-0.08	7.563 +/-0.11
DIPPA	7.838 +/-0.09	7.765 +/-0.09	
N-MPPP	8.621 +/-0.09	8.423 +/-0.08	
BRL 52537	8.843 +/-0.09	8.702 +/-0.07	
ICI 204488	8.025 +/-0.08	8.255 +/-0.12	
ICI 199441	8.587 +/-0.07	9.189 +/-0.05	9.188 +/-0.05
GR8969	8.819 +/-0.08	9.492 +/-0.06	9.506 +/-0.05
(-)U50488	8.600 +/-0.09	8.910 +/-0.09	
Beta-NNTA	9.395 +/-0.13	9.354 +/-0.09	
6' GNTI	8.252 +/-0.08	7.489 +/-0.23	
Diprenorphine	8.615 +/-0.11	8.404 +/-0.10	
Butorphanol	8.611 +/-0.09	8.249 +/-0.19	
Nalbuphine	6.735 +/-0.14	7.240 +/-0.16	
Cyclazocine	8.771 +/-0.09	8.804 +/-0.14	
RB 48	7.87 +/-0.07	6.44 +/-0.09	7.221 +/-0.06
RB 64	7.94 +/-0.07	6.38+/-0.06	6.824 +/-0.06
RB 50	6.89 +/-0.12	5.03 +/-0.13	

RB 65	6.56 +/-0.13	5.08 +/-0.22	
RB 59	6.98 +/-0.10	4.97 +/-0.12	5.400 +/-0.70
RB 55-2	6.74 +/-0.08	5.19 +/-0.15	
RB 55-1	6.85 +/-0.09	5.49 +/-0.15	
RB 55	7.32 +/-0.09	6.42 +/-0.07	6.286 +/-0.14
Salvinorin B	6.89 +/-0.10	6.30 +/-0.05	
Dyn 1-13	8.497 +/-0.04	6.94 +/-0.09	6.979 +/-0.16
Dyn 1-9	7.636 +/-0.07	6.415 +/-0.13	6.439 +/-0.12
Dyn 1-11	8.263 +/-0.07	6.594 +/-0.12	6.816 +/-0.22
Dyn 1-8	7.249 +/-0.07	6.574 +/-0.09	6.344 +/-0.14
Dyn A	8.149 +/-0.06	6.590 +/-0.12	6.825 +/-0.09

Compound Synthesis Procedures

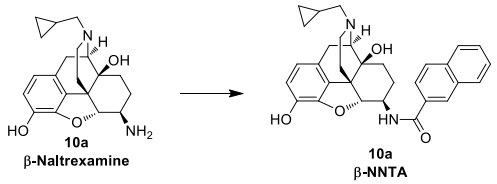

β-NNTA (11a).[5b] An oven-dried 2-dram vial with a sepcap, cooled under N_2, was charged with **10a** (40.0 mg, 0.117 mmol), dry $CHCl_3$ (0.8 mL) and dry pyridine (25.0 µL, 0.309 mmol). The solution was cooled to 0 °C and 2-naphthoyl chloride (33.4 mg, 0.175 mmol) was added in $CHCl_3$ (0.5 mL) dropwise via syringe over 20 min down the wall of the vial. The solution was stirred at 0 °C for 0.5 h, then at room temperature for 5 h. The solution was concentrated under a stream of N_2 to a residue that was dissolved in MeOH (1 mL) and K_2CO_3 (81 mg, 0.59 mmol) was added in one portion. The mixture was stirred for 2 h then brine (5 mL) and H_2O (5 mL) were added, the pH of the solution was adjusted to 7-8 with saturated NH_4Cl solution and extracted with CH_2Cl_2 (3 x 10 mL). The organic extracts were pooled, washed with H_2O (2 x 20 mL) and brine (20 mL), dried ($NaSO_4$) and filtered. Concentration under vacuum provided 67.3 mg of a yellow residue. Purification by silica (10 g) flash column (1.5 x 16 cm) chromatography, eluting with 97:2.5:0.5 (150 mL) CH_2Cl_2/MeOH/concd $NH_4OH_{(aq)}$ yielded 46.9 mg (81%) of the title compound as a white solid: **^{1}H NMR** (400 MHz, acetone-d_6) δ 8.53 (s, 1H), 8.18-7.82 (m, 5H), 7.65-7.54 (m, 2H), 6.69 (d, *J* = 8.0 Hz; 1H), 6.58 (d, *J* = 8.0 Hz; 1H), 4.97 (br s, 1H), 4.69 (d, *J* = 7.3 Hz; 1H), 4.03 (dd, *J* = 5.5, 11.8 Hz; 1H), 3.16-3.04 (m, 2H), 2.83 (d, *J* = 13.1 Hz; 2H), 2.75-2.61 (m, 2H), 2.45 (dd, *J* = 6.8, 12.8 Hz; 1H), 2.39 (dd, *J* = 6.8, 12.8 Hz; 1H), 2.27 (ddd, *J* = 4.8, 12.3, 12.3 Hz; 1H), 2.15 (ddd, *J* = 2.3, 11.8, 11.8 Hz; 1H), 2.03-1.91 (m, 1H), 1.77-1.65 (m, 1H), 1.63-1.44 (m, 2H), 1.4 (d, *J* = 11.5 Hz; 1H), 0.97-0.84 (m, 1H), 0.60-0.44 (m, 2H), 0.24-0.08 (m, 2H); **LC-MS** (ESI+) m/z: $[M + H]^+$ Calcd for $C_{31}H_{33}N_2O_4$ 497.60; Found 497.34.

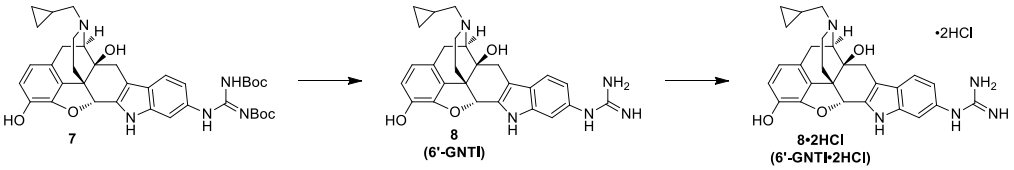

***6'-Guanidino*-17-(cyclopropylmethyl)-6,7-didehydro-4,5α-epoxy-3,14-dihydroxyindolo[2',3':6,7]morphinan (8, 6'-GNTI).**[2,3b] A tared 50 mL flask was charged with di-Boc-guanidine **7** (367 mg, 0.546 mmol) and TFA (4.5 mL). The grey solution was stirred for 75 min, then concentrated to dryness from toluene (1 x 10 mL and 2 x 5 mL) to afford 442 mg of an off-white solid, to which was added MeOH (4.5 mL). The slight suspension was filtered under positive pressure through a plug (0.8 x 1 cm) of Celite in a pipet (4 mL) and the clear filtrate was added in equal portions to three auto sampler vials. Purification of each portion was accomplished by reverse phase preparative-LC (Agilent) using a phenyl-cyclohexyl capped column, eluting at 70 mL/min, detecting at 232 and 288 nm; solvent A = 99.95:0.05 H_2O/TFA, solvent B = MeOH; method: 10→70% B (0-9 min; linear gradient), 70→100% B (9-9.01 min; linear gradient) and 100% B (9.01→10 min; isocratic). Pooled all appropriate fractions, concentrated under vacuum and azeotropically dried the remaining residue with toluene (3 x 5 mL). Obtained 328 mg of the bis-TFA salt as a white solid. The solid was dissolved in MeOH (30 mL), MP-carbonate resin (*ca.* 200 mg, 2.5-3.5 mmol/g) was added and the mixture was stirred until a pH of 7-8 (pH paper) was achieved (10-15 min). The resin was removed by vacuum filtration (fine porosity sintered glass funnel; washed resin with 5 mL MeOH) and the filtrate was concentrated under vacuum to leave 220 mg (85%) of 6'-GNTI freebase as a white solid (^{1}H and ^{13}C NMR analyses performed). The majority of the solid (200 mg, 0.424 mmol) was dissolved in MeOH (10 mL) and HCl (220 µL, 4 M solution in 1,4-dioxane, 0.88 mmol) was added dropwise over 1 min. After stirring for 10 min the solution was concentrated to a volume of 3-4 mL on a rotary evaporator and then diluted (while stirring) with 35-40 mL of Et_2O. The resulting precipitate was collected by vacuum filtration (medium porosity sintered glass funnel). Further drying under high vacuum (12 h) yielded 201 mg (87%) of the title compound bis-hydrochloride salt as a white powder: **^{1}H NMR** (400 MHz, methanol-d_4) δ 7.45 (d, *J* = 8.4 Hz; 1H), 7.21 (d, *J* = 1.6 Hz; 1H), 6.83 (dd, *J* = 1.8, 8.3 Hz; 1H), 6.51 (d, *J* = 8.3 Hz; 1H), 6.49 (d, *J* = 8.3 Hz; 1H), 5.54 (s, 1H), 3.39 (d, *J* = 6.5 Hz; 1H), 3.17 (d, *J* = 18.6 Hz; 1H), 2.85-2.71 (m, 3H), 2.62 (d, *J* = 15.7 Hz; 1H), 2.53-2.41 (m, 2H), 2.41-2.29 (m, 2H), 1.82-1.68 (m, 1H), 1.00-0.89 (m, 1H), 0.63-0.52 (m, 2H), 0.25-0.15 (m, 2H); **^{1}H NMR** (400 MHz, DMSO-d_6) δ 7.30 (d, *J* = 8.4 Hz; 1H), 6.70 (d, *J* = 1.1 Hz; 1H), 6.64 (dd, *J* = 1.7, 8.3 Hz; 1H), 6.50 (d, *J* = 8.1 Hz; 1H), 6.47 (d, *J* = 8.1 Hz; 1H), 5.49 (s, 1H), 4.72 (br s, 1H), 3.27 (d, *J* = 6.3 Hz; 1H), 3.06 (d, *J* = 18.6 Hz; 1H), 2.79-2.63 (m, 3H), 2.46-2.34 (m, 3H), 2.31 (ddd, *J* = 4.9, 12.5, 12.5 Hz; 1H), 2.15 (ddd, *J* = 2.9, 11.9, 11.9 Hz; 1H), 1.59 (d, *J* = 11.3 Hz; 1H), 0.96-0.82 (m, 1H), 0.58-0.43 (m, 2H), 0.20-0.10 (m, 2H); **^{13}C NMR** (100 MHz, methanol-d_4) δ 158.6, 145.4, 143.8, 139.0, 133.4, 131.8, 130.7, 127.9, 124.6, 120.9, 119.9, 119.3, 118.1, 111.6, 110.3, 85.4, 74.6, 63.7, 60.7, 45.1, 32.9, 29.9, 24.2, 10.4, 4.8, 4.3; **^{13}C NMR** (100 MHz, DMSO-d_6) δ 154.7, 143.0, 139.8, 137.2, 131.1, 129.8, 124.2, 123.7, 118.9, 118.2, 116.7, 116.5, 110.1, 107.1, 83.9, 72.1, 61.6, 58.6, 47.2, 43.3, 31.1, 28.7, 22.7, 9.2, 3.8, 3.4; **LC-MS** (ESI+) m/z: $[M + H]^+$ Calcd for $C_{27}H_{30}N_5O_3$ 472.24; Found 472.57.

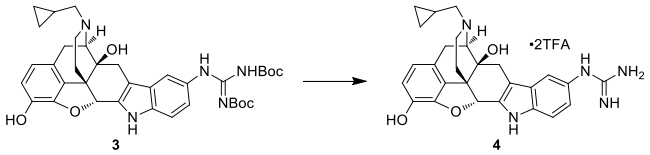

***5'-Guanidino*-17-(cyclopropylmethyl)-6,7-didehydro-4,5α-epoxy-3,14-dihydroxyindolo[2',3':6,7]morphinan (4, 5'-GNTI).**[1,2,3] To a tared 50 mL flask, containing TFA (3.5 mL, ~100 equiv.), was added **3** (319 mg, 0.475) in portions over 1-2 min. The resulting grey-green solution was stirred for 45 min and then concentrated to dryness from toluene (3 x 5 mL) and $CHCl_3$ (5 mL). Continued drying under high vacuum gave *ca.* 400 mg of an off-white solid. Addition of 95:5 MeOH/DMF (~5 mL) gave a slight suspension, which was filtered under positive pressure through a plug of Celite (0.5 x 2 cm) in a pipet (5¾ inch). The clear filtrate was added in equal portions to five auto sampler vials (1.6 mL capacity) and purified by reverse-phase preparative-LC with a phenyl-hexyl column, eluting at 70 mL/min, and detecting at 222 and 274 nm; solvent A = 99.95:0.05 H_2O/TFA, solvent B = MeOH; method: 10→100% B (0→9 min; linear gradient) and 100% B (9→10 min; isocratic). Obtained 298 mg (90%) of the title compound (**4•2TFA**) as a white solid: $[\alpha]_D^{25}$ –176.6 (*c* 0.53, MeOH); **^{1}H NMR** (400 MHz, DMSO-d_6) δ 11.56 (s, 1H), 9.63 (s, 1H), 9.26 (br s, 1H), 8.96 (br s, 1H), 7.42 (d, *J* = 8.6 Hz; 1H), 7.26-7.11 (m, 5H), 6.95 (dd, *J* = 1.8, 8.6 Hz; 1H), 6.62 (d, *J* = 8.1 Hz; 1H), 6.58 (d, *J* = 8.1 Hz; 1H), 6.39 (br s, 1H), 5.71 (s, 1H), 4.08 (d, *J* = 6.3 Hz; 1H), 3.45 (d, *J* = 19.6 Hz; 1H), 3.38 (dd, *J* = 7.0, 13.9 Hz; 1H), 3.24 (dd, *J* = 6.9, 19.8 Hz; 1H), 3.12 (d, *J* = 11.7 Hz; 1H), 3.00-2.90 (m, 1H), 2.95 (d, *J* = 15.9 Hz; 1H), 2.79-2.56 (m, 2H), 1.83 (d, *J* = 11.4 Hz; 1H), 1.16-1.04 (m, 1H), 0.77-0.69 (m, 1H), 0.68-0.59 (m, 1H), 0.54-0.40 (m, 2H); **^{1}H NMR** (400 MHz, methanol-d_4) δ 7.46 (d, *J* = 8.5 Hz; 1H), 7.36 (d, *J* = 1.8 Hz; 1H), 7.04 (dd, *J* = 2.0, 8.6 Hz; 1H), 6.68 (d, *J* = 8.2 Hz; 1H), 6.65 (d, *J* = 8.2 Hz; 1H), 5.74 (s, 1H), 4.23 (d, *J* = 6.5 Hz; 1H), 3.44-3.35 (m, 2H), 3.20 (dd, *J* = 4.2, 12.6 Hz; 1H), 3.05-2.97 (m, 1H), 3.01 (d, *J* = 16.2 Hz; 1H), 2.94 (dd, *J* = 3.7, 12.9 Hz; 1H), 2.77 (ddd, *J* = 4.8, 13.4, 13.4 Hz; 1H), 2.73 (d, *J* = 16.1 Hz; 1H), 1.98 (dd, *J* = 2.6, 13.5 Hz; 1H), 1.22-1.11 (m, 1H), 0.93-0.85 (m, 1H), 0.83-0.75 (m, 1H), 0.60-0.50 (m, 2H); **^{13}C NMR** (100 MHz, methanol-d_4) δ 159.0, 145.0, 142.3, 138.4, 132.7, 130.4, 128.7, 127.1, 122.7, 122.4, 120.8, 119.6, 118.2, 114.0, 110.2, 85.0, 73.7, 63.8, 59.1, 48.3, 47.8, 30.4, 29.9, 25.2, 7.0, 6.4, 3.5; **HRMS** (ESI-TOF) m/z: $[M + H]^+$ Calcd for $C_{27}H_{30}N_5O_3$ 472.2349; Found 472.2349

References (Supplemental)

(1) (a) Jones, R. M.; Hjorth, S. A.; Schwartz, T. W.; Portoghese, P. S. *J. Med. Chem.* **1998**, *41*, 4911–4914. (b) Stevens, W. C., Jr.; Jones, R. M.; Subramanian, G.; Metzger, T. G.; Ferguson, D. M.; Portoghese, P. S. *J. Med. Chem.* **2000**, *43*, 2759–2769.
(2) A κ-opioid receptor agonist: Sharma, S. K.; Jones, R. M.; Metzger, T. G.; Ferguson, D. M.; Portoghese, P. S. *J. Med. Chem.* **2001**, *44*, 2073–2079.
(3a) Portoghese, P. S.; Jones, R. M. Kappa (OP_2) Opioid Receptor Antagonist. U.S. Patent 6,500,824 B1, Dec 31, 2002.
(3b) Portoghese, P. S.; Jones, R. M.; Sharma, S. K. Therapeutic Compounds and Methods. U.S. Patent 7,232,829 B2, Jun 19, 2007.
(5b) Le Naour, M.; Lunzer, M. M.; Powers, M. D.; Portoghese, P. S. *J. Med. Chem.* **2012**, *55*, 670–677.